

## Simultaneous quantification of alternatively spliced transcripts in a single droplet digital PCR reaction

Bing Sun, Lian Tao, and Yun-Ling Zheng

Cancer Prevention and Control Program, Lombardi Comprehensive Cancer Center, Georgetown University Medical Center, Washington DC

*BioTechniques* 56:319-325 (June 2014) doi 10.2144/000114179

Keywords: RNA alternative splicing; telomere; telomerase; hTERT; real-time PCR; qPCR; droplet digital PCR; ddPCR

Human telomerase reverse transcriptase (hTERT) is an essential component required for telomerase activity and telomere maintenance. Several alternatively spliced forms of hTERT mRNA have been reported in human primary and tumor cells. Currently, however, there is no sensitive and accurate method for the simultaneous quantification of multiple alternatively spliced RNA transcripts, such as in the case of hTERT. Here we show droplet digital PCR (ddPCR) provides sensitive, simultaneous digital quantification in a single reaction of two alternatively spliced single deletion hTERT transcripts ( $\alpha$ -/ $\beta$ + and  $\alpha$ +/ $\beta$ -) as well as the opportunity to manually quantify non-deletion ( $\alpha$ +/ $\beta$ +) and double deletion ( $\alpha$ -/ $\beta$ -) transcripts. Our ddPCR method enables direct comparison among four alternatively spliced mRNAs without the need for internal standards or multiple primer pairs specific for each variant as real-time PCR (qPCR) requires, thus eliminating potential variation due to differences in PCR amplification efficiency.

Humans synthesize ~150,000 different proteins from 25,000–30,000 genes by alternative splicing. It is estimated that more than 70% of human protein-coding genes produce multiple alternatively spliced mRNA transcripts (1). When these mRNAs are translated, they produce an array of proteins with diverse and even antagonistic functions. A large proportion of human genetic disorders are the result of abnormal splicing, with abnormal splicing variants thought to even contribute to the development of cancer (2,3). Given the importance of alternative splicing in regulating cellular function, accurate quantification of multiple alternatively spliced transcripts could facilitate the discovery of new biomarkers for clinical applications and thus enhance our understanding of the role of alternative splicing in health and disease.

Next-generation sequencing seems to be the best approach for profiling

expression patterns of alternative splicing variants, but its application is limited due to its high cost and the large amount of RNA required. Specific microarrays (e.g., Affymetrix exon microarray, ExonHit) have been developed for profiling splicing variants, but these platforms cannot distinguish transcripts containing either exon A or B alone from those containing both exons.

Approximately 20 alternatively spliced variants of human telomere reverse transcriptase (hTERT) have been reported, and 4 of these transcripts ( $\alpha$  deletion:  $\alpha$ -/ $\beta$ +;  $\beta$  deletion:  $\alpha$ +/ $\beta$ -;  $\alpha$ +/ $\beta$  double deletion:  $\alpha$ -/ $\beta$ -; no-deletion:  $\alpha$ +/ $\beta$ +) are commonly present in most tumor tissues and may serve as specific markers for cancer diagnosis, prediction of clinical outcome, or as drug targets (4–10). The  $\alpha$ -deletion transcript has a 36 nucleotide deletion within the conserved reverse transcriptase motif and is a dominant-negative inhibitor

of telomerase activity (5). The  $\beta$ -deletion transcript has a 182 nucleotide deletion, leading to a truncated protein lacking the conserved reverse transcriptase motifs and resulting in a catalytically inactive telomerase (6,7). Only the full-length hTERT transcript has been shown to be associated with telomerase activity. Telomerase activation has been shown to be associated with carcinogenesis. Over 90% of tumor tissues have increased telomerase activity comparing to adjacent normal tissues (8,9). However, the level of telomerase activity in the tumor tissues was not correlated with hTERT transcript levels, which may be due to post-transcriptional processing resulting in the formation of alternatively spliced mRNAs. This may serve as a mechanism for regulating telomerase activity, since the relative quantities of each mRNA may determine the overall enzyme activity. Several real-time PCR (qPCR)-based assays for the enumeration of

### METHOD SUMMARY

Using a single pair of primers and two probes for the telomerase enzymatic component hTERT, four alternatively spliced mRNA transcripts (single deletions  $\alpha$ -/ $\beta$ + and  $\alpha$ +/ $\beta$ -, double deletion  $\alpha$ -/ $\beta$ -, and non-deletion  $\alpha$ +/ $\beta$ +) are simultaneously and accurately quantified using a novel methodology based on counting data from a single droplet digital PCR (ddPCR) reaction.

common hTERT splice variants have been developed and used to study human cancer tissues to determine splicing patterns, but these assays failed to identify a consistent correlation between the level of telomerase activity and the level of hTERT transcripts (10–14). The qPCR methods used previously have limited sensitivity of quantification for some of the alternatively spliced forms that are expressed at very low levels. In general, normal tissues were shown to express very little or no hTERT, while tumor tissues only express low levels of hTERT transcripts. Among all of the transcript variants, double deletion and  $\alpha$ -deletion transcripts are usually the lowest, if co-expressed. Another confounding factor was the use of multiple primer pairs for each variant where multiple qPCR reactions had to be carried out together with individual internal standards. Variations in PCR amplification efficiency in this case compromise the quantification accuracy, making the comparison less reliable. Here, we demonstrated a method based on droplet digital PCR (ddPCR) for the simultaneous quantification of the four major alternatively spliced forms of hTERT using just one pair of primers in a single ddPCR reaction that results in high sensitivity without the need for internal standards.

## Materials and methods

All of the cell lines (ovarian cancer OVCar-3, osteosarcoma SAOS-2 and U2OS, breast

cancer MCF-7, lung fibroblast WI-38, and endometrium adenocarcinoma HEC-1-A) used in this study were obtained from ATCC (Manassas, VA) or from our institution's cell culture core facility, and were cultured in the media recommended by the providers. The forward-primer for hTERT cDNA amplification (5'-GCCTGAGCTGTACTTTGTCA-3'; PCR-F in Figure 1) was designed to bind upstream of the  $\alpha$ -deletion splicing site. The reverse-primer (PCR-R in Figure 1) is downstream of the  $\beta$ -deletion splicing site with sequence 5'-CAGCGTGAGAGGATGGAG-3'. A dual-labeled  $\alpha$ -deletion probe was designed with FAM as the fluorescent indicator and ZEN-Iowa Black as the quencher (Figure 1). The probe sequence (5'-FAM/TACTTTGTC/ZEN/AAGGACAGGCTCACG/IABk/-3') overlapped partially with the transcript before and after the deleted region; thus, in theory, the probe should specifically recognize  $\alpha$ -deletion transcripts. A  $\beta$ -deletion probe was designed the same way as shown in Figure 1 (5'-HEX/CTTCAAGAG/ZEN/CCAGTCCTACGTC/IABk/-3), except HEX was used as the fluorescent indicator. A non-deletion  $\beta$  probe was selected with a sequence in the deleted region (5'-6-FAM/CTCTACCTT/ZEN/GACAGACCTCCAGC/IABkFQ/-3'). GAPDH (forward primer 5'-ATTCCACCCATGGCAAATTC-3', reverse primer 5'-TGGGATTTCCATTGATGACAAG-3', and probe 5'-/HEX/CAAGCTTCCCGTTCTCAGCC/IABkFQ/-3) was used as internal control for normal-

ization for the comparison between samples. All primers and probes were synthesized by Integrated DNA Technologies, Inc. (Coralville, IW).

Total RNA from cultured tumor cell lines and fibroblasts was extracted with the TRIzol total RNA extraction kit (Life Technologies, Grand Island, NY). One  $\mu$ g total RNA was used for cDNA synthesis in a 10  $\mu$ L reaction using the iScript Select cDNA synthesis kit (Bio-Rad, Hercules, CA) and 19 nucleotide oligo dT + A/G/C to ensure 1:1 reverse transcription. To serve as positive controls for accurate identification and quantification of each variant, synthetic hTERT DNA fragments of the four splice forms were amplified by PCR using PCR-F and another reverse primer (5'-GCCTGAGCTGTACTTTGTCA-3') downstream of PCR-R, and then further cloned into the pCR4-TOPO TA vector (Life Technologies, Grand Island, NY), and sequence verified by Sanger DNA sequencing (Genewiz, Germantown, MD). To check the detection specificity, each one of four cloned variants were first added alone to a ddPCR reaction, and the 2-D results are shown in Figure 2. As expected, droplets with each variant were detected and represented in the upper left, lower right, upper right, and lower left quadrant for  $\alpha$  deletion (Figure 2A),  $\beta$  deletion (Figure 2B),  $\alpha$ & $\beta$  double deletion (Figure 2C,) and non-deletion (Figure 2D), respectively. The droplets containing the non-deletion hTERT variant appeared slightly higher in the 2-D

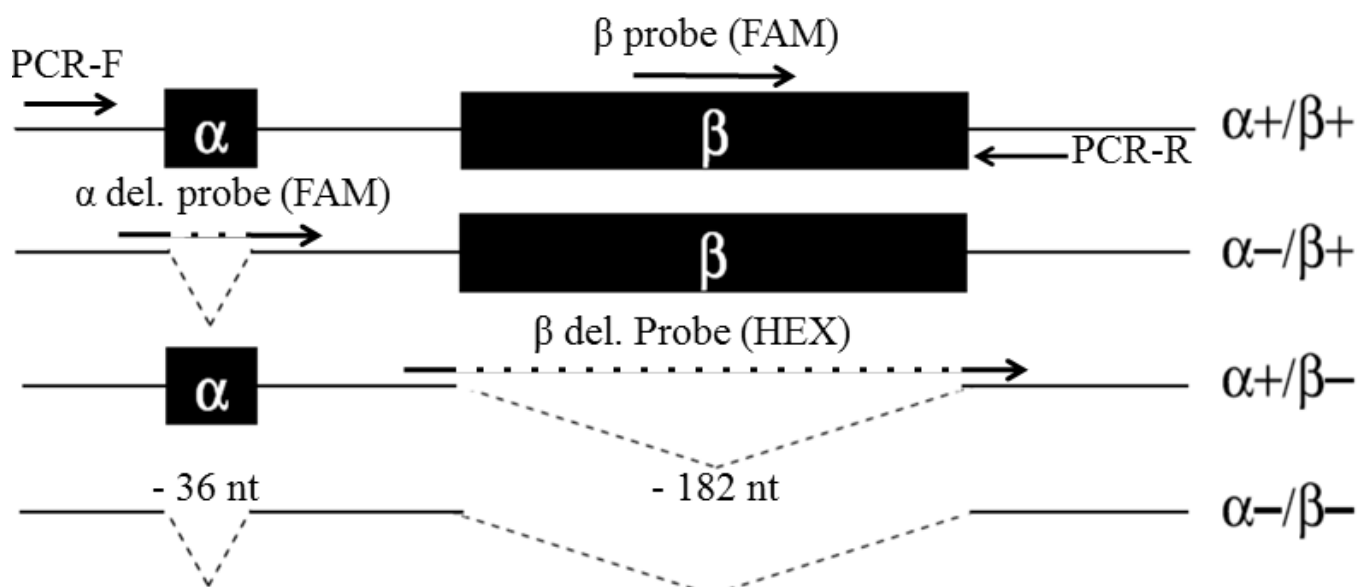


**Figure 1.** hTERT mRNA  $\alpha$ -deletion ( $\alpha$ -/ $\beta$ +),  $\beta$ -deletion ( $\alpha$ +/ $\beta$ -) and  $\alpha$ -/ $\beta$ - double deletion. Deleted regions are designated by dashed lines.

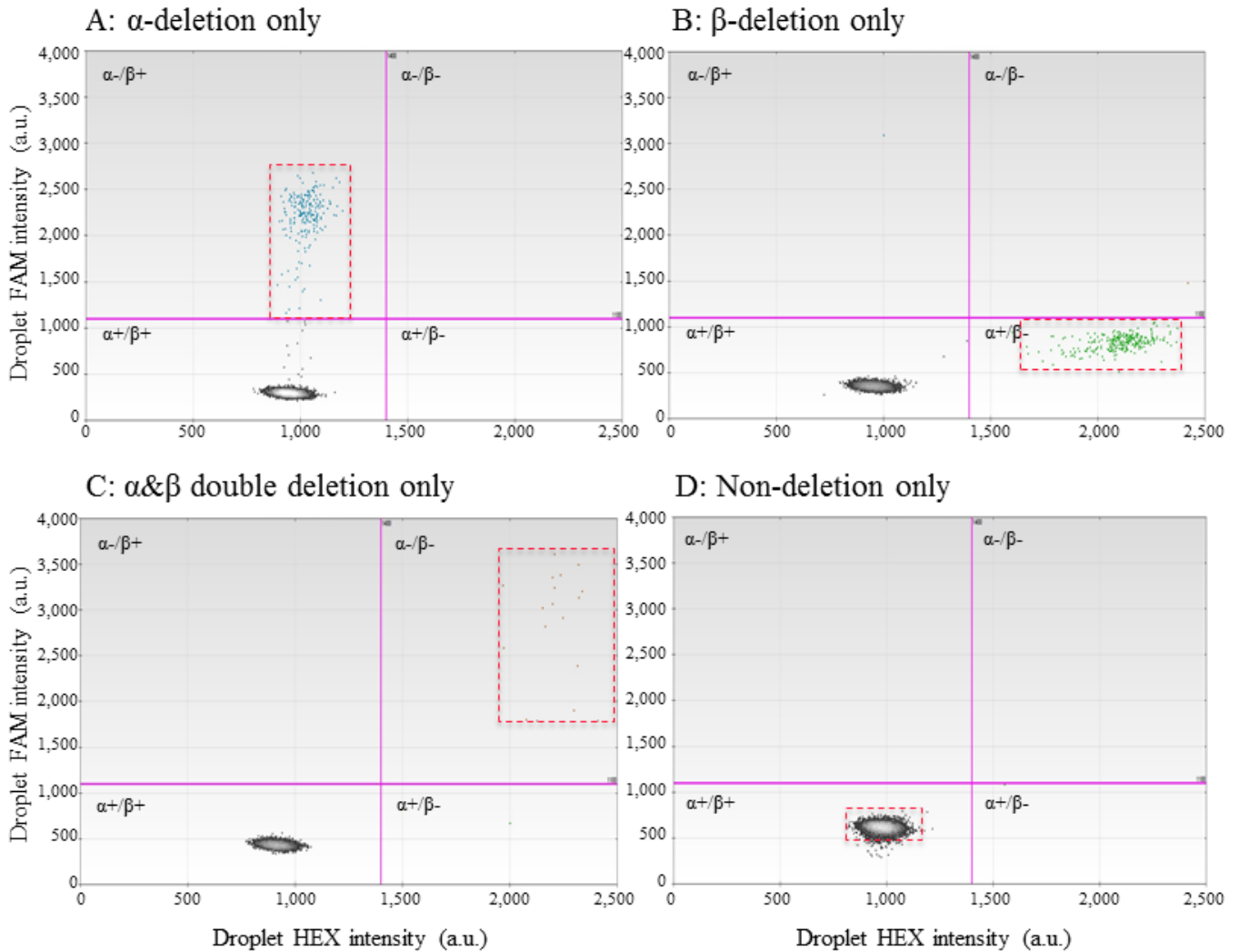


**Figure 2.** 2-D display of positive droplets after ddPCR amplification of cloned positive controls for each individual splice form. FAM-positive and HEX-positive droplets are shown from droplet digital PCR reactions containing both  $\alpha$ -deletion (FAM) and  $\beta$ -deletion (HEX) probes. FAM-positive droplets (i.e.,  $\alpha$ -/ $\beta$ +) are presented in the upper left quadrant. HEX-positive droplets (i.e.,  $\alpha$ +/ $\beta$ -) are presented in the lower right quadrant. Double-positive droplets ( $\alpha$ -/ $\beta$ - in dashed rectangle) are presented in the upper right quadrant. Weak FAM-positive ( $\alpha$ +/ $\beta$ + in dashed rectangle) or negative droplets are shown in the lower left quadrant.

plot relative to the negative droplets in the lower left quadrant in Figure 2C. A series of experiments was carried out combining two, three, or four cloned hTERT variants in one ddPCR reaction to simulate samples from cells or tissues. To demonstrate the presence of  $\alpha$ -deletion and  $\beta$ -deletion in the same droplets, cloned  $\alpha$ -deletion and  $\beta$ -deletion templates were titrated and used at relatively high concentrations.

For ddPCR, the reaction mixture was assembled from a 2 $\times$  ddPCR Supermix (Bio-Rad), plus primers (250 nM each), probes (125 nM) and 1  $\mu$ L cDNA in a final volume of 20  $\mu$ L for hTERT. cDNA was diluted 1:2,000 for GAPDH expression quantification in a separate tube. Droplet generation, PCR reaction, and detection were carried out according to

manufacturer's instruction (15). Briefly, each assembled ddPCR reaction mixture was then loaded into the sample well of an eight-channel droplet generator cartridge (Bio-Rad). A 70  $\mu$ L volume of droplet generation oil was loaded into the oil well for each channel. The cartridge was placed into the droplet generator (Bio-Rad) for droplet generation (up to 20,000 per reaction). The droplets that collected in the droplet well in the cartridge were then manually transferred with a multichannel pipette to a 96-well PCR plate. The plate was heat-sealed with a foil seal and then placed on a conventional thermal cycler (T100, Bio-Rad). After PCR, the 96-well PCR plate was loaded on the droplet reader (QX100, Bio-Rad), which automatically reads the droplets from each well of the

plate. Instead of using auto-analysis after data acquisition with QuantaSoft analysis software, manual selection of "+/-," "-/+," and "-/-" counts was done using the Lasso function in the 2-D plots. The counts were then used by the software to calculate the copy numbers of  $\alpha$ -deletion (FAM-positive),  $\beta$ -deletion (HEX-positive),  $\alpha$ & $\beta$  double deletion or combined single  $\alpha$ - and  $\beta$ -deletions (FAM- and HEX-double positive), and non-deletion forms (weak FAM-positive) in the four quadrants. A second ddPCR reaction with the same primer pair plus non-deletion  $\beta$  probe instead of  $\alpha$ -deletion probe (FAM-labeled, Figure 1) and  $\beta$ -deletion probe (HEX) was also performed to help assess the possibility of the presence of both single  $\alpha$ -deletion and single  $\beta$ -deletion in the

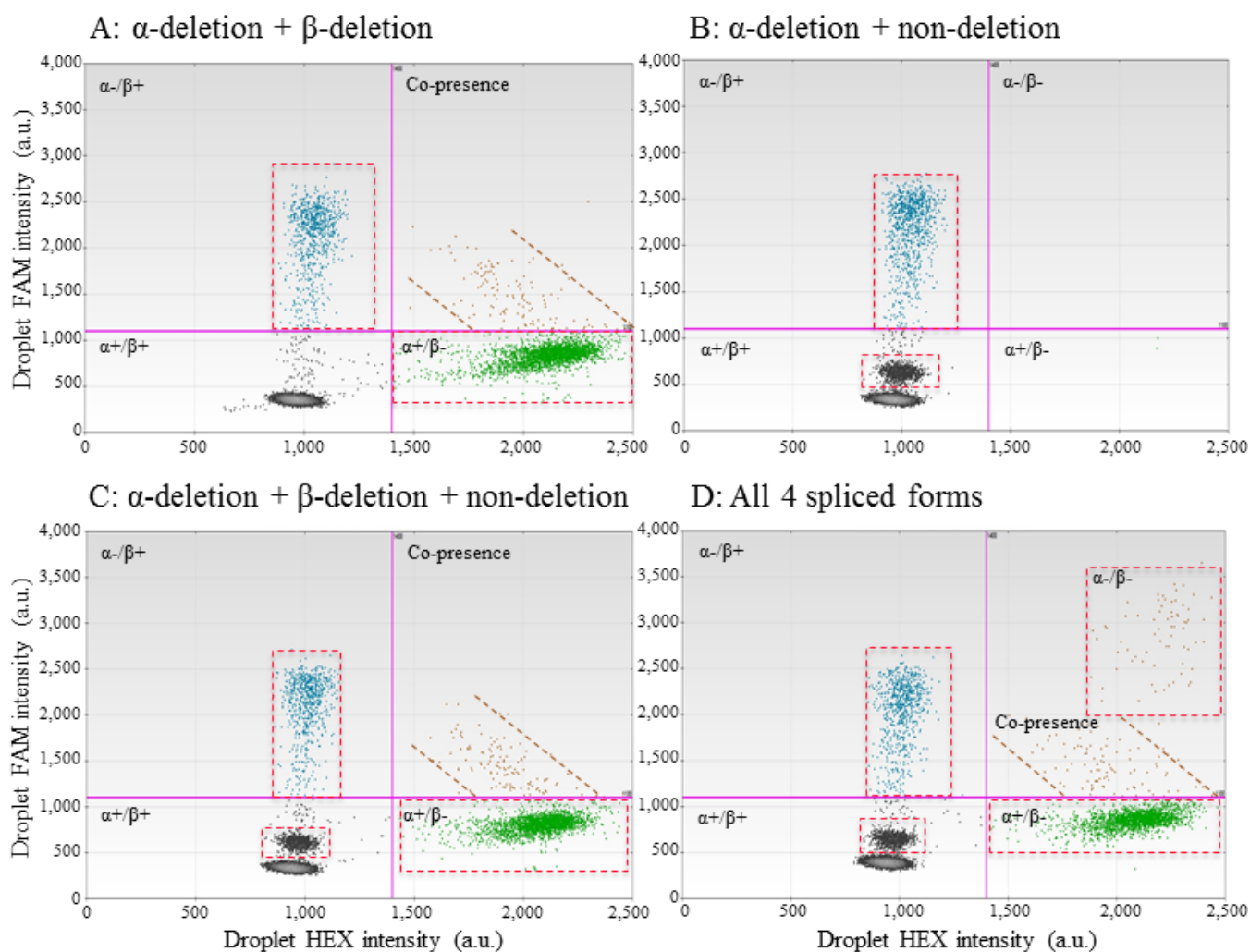


**Figure 3.** 2-D display of positive droplets after ddPCR amplification of cloned positive controls in combination (A)–(D), with FAM-positive in y-axis and HEX-positive in x-axis, in a single droplet digital PCR reaction containing both  $\alpha$ -deletion (FAM) and  $\beta$ -deletion (HEX) probes. FAM-positive droplets (i.e.,  $\alpha$ -/ $\beta$ +) are presented in the upper left quadrant. HEX-positive droplets (i.e.,  $\alpha$ +/ $\beta$ -) are presented in the lower right quadrant. Double-positive droplets ( $\alpha$ -/ $\beta$ - in dashed rectangle and the co-presence of  $\alpha$ - and  $\beta$ -deletion transcripts between dashed lines) are presented in the upper right quadrant. Weak FAM-positive ( $\alpha$ +/ $\beta$ +) or negative droplets are in the lower left quadrant.

same droplet, which may interfere with the accurate quantification of  $\alpha$ & $\beta$  double deletion transcripts.

## Results and discussion

During our initial experiments, it was observed that, in addition to the quantification of  $\alpha$ -deletion ( $\alpha$ -/ $\beta$ +) in the left upper quadrant, such as in Figure 4B and 4C) and  $\beta$ -deletion ( $\alpha$ +/ $\beta$ - in the right lower quadrant, such as in Figure 4 A–C), a group of weak FAM-positive droplets was detected just above the negative droplets in the lower left quadrant (as shown in dashed rectangles of Figure 4A–C). We speculated that these droplets contain non-deletion hTERT transcripts ( $\alpha$ +/ $\beta$ +) that were detected

with weak FAM fluorescent signals due to inefficient hydrolysis of the  $\alpha$ -deletion probe, since the  $\alpha$ -deletion probe probably partially hybridized to the non-deletion form at the set annealing temperature during PCR. To confirm this, we performed an experiment using cloned  $\alpha$ -deletion plasmids plus the cloned non-deletion plasmid as templates for ddPCR. Compared to the results obtained with the cloned  $\alpha$ -deletion plasmid alone as shown in Figure 2A, a new group of weak FAM-positive droplets can be seen in the lower left quadrant (dashed rectangle) after adding cloned non-deletion hTERT fragments to the cloned  $\alpha$ -deletion (Figure 3, B–D). The quantification accuracy for the non-deletion form was confirmed by subtraction of  $\alpha$ -deletion counts from

non- $\beta$  deletion counts obtained from the experiments with the non-deletion  $\beta$  probe and  $\beta$ -deletion probe. Although the detection of the non-deletion transcript by a deletion probe in this case is coincidental and may not occur in all situations, proper probe design and optimization may allow the same detection of a non-deletion transcript with a deletion probe in the case of other alternatively spliced genes.

FAM- and HEX-double positive droplets were detected, as shown in the upper right quadrants in Figure 4B and 4C (dashed rectangles). There are two possibilities for this observation: (i) the presence of  $\alpha$ -deletion and  $\beta$ -deletion transcripts in the same droplet or (ii) the presence of a transcript with  $\alpha$ & $\beta$  double deletion. In

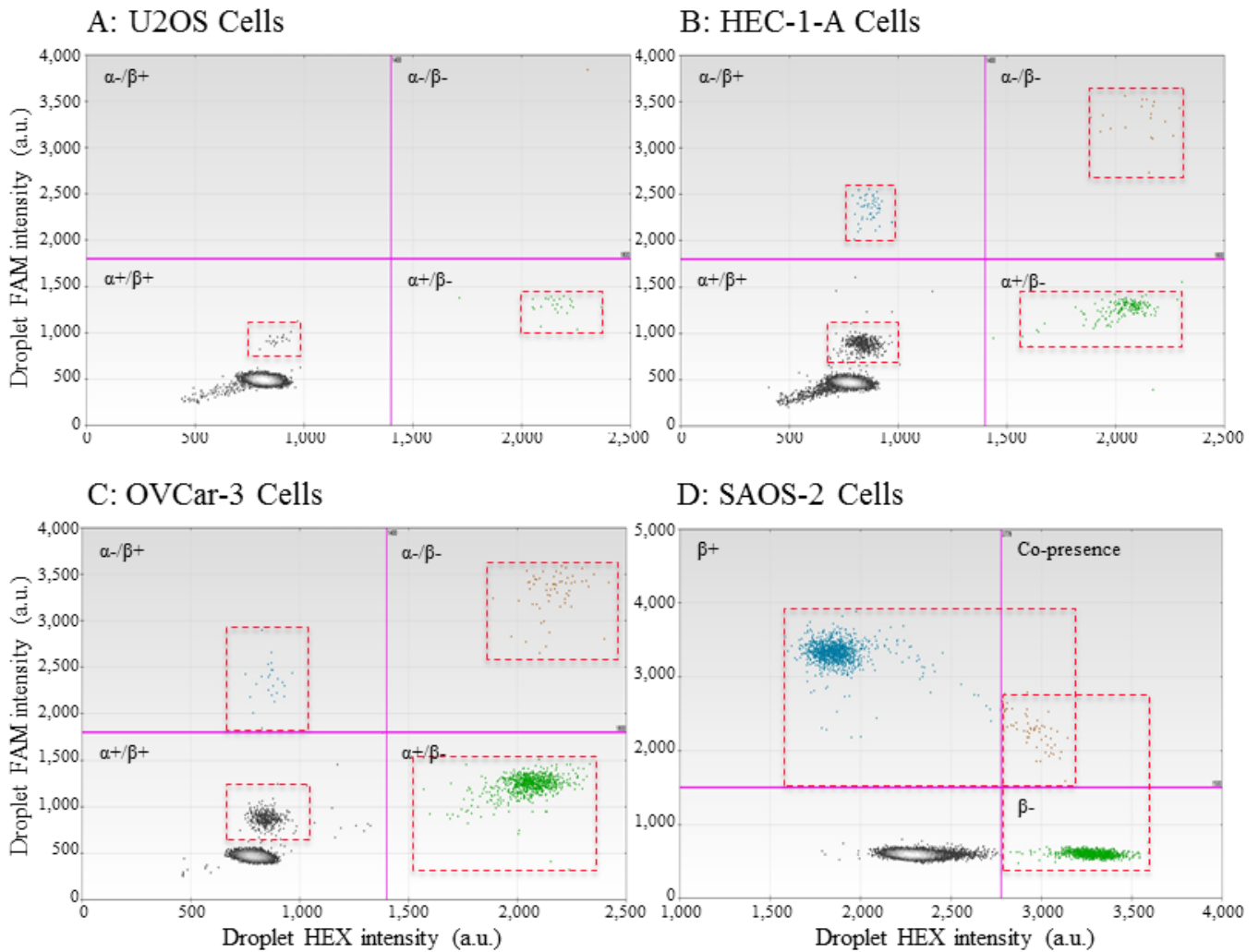


**Figure 4. 2-D display of positive droplets after ddPCR amplification with FAM-positive in y-axis and HEX in x-axis.** (A–C): Detection of three deletion ( $\alpha$ -/ $\beta$ +,  $\alpha$ +/ $\beta$ -,  $\alpha$ -/ $\beta$ -) and non-deletion ( $\alpha$ +/ $\beta$ +) forms of hTERT in a single droplet digital PCR reaction with  $\alpha$ -deletion (FAM) and  $\beta$ -deletion (HEX) probes. FAM-positive droplets (i.e.,  $\alpha$ -/ $\beta$ +) are presented in the upper left quadrant. HEX-positive droplets (i.e.,  $\alpha$ +/ $\beta$ -) are presented in the lower right quadrant. Double-positive droplets (i.e.,  $\alpha$ -/ $\beta$ - or the presence of both single  $\alpha$ - and  $\beta$ -deletions) are presented in the upper right quadrant. Weak FAM-positive ( $\alpha$ +/ $\beta$ +) or negative droplets are in the lower left quadrant. (D): Detection of  $\beta$ -deletion and non- $\beta$  deletion in a single droplet digital PCR reaction with non-deletion  $\beta$  (FAM) and  $\beta$ -deletion (HEX) probes. FAM-positive droplets (i.e.,  $\beta$ +) are presented in the dashed rectangle in upper half. HEX-positive droplets (i.e.,  $\beta$ -) are presented in the dashed rectangle on the right. Double-positive droplets [i.e., presence of both non- $\beta$  deletion ( $\beta$ +) and  $\beta$ -deletion ( $\beta$ -)] are presented in the upper right quadrant.

the former case, two independent PCR amplifications, one using the  $\alpha$ -deletion transcript as template and the other using the  $\beta$ -deletion transcript as template, would have occurred simultaneously in the same droplet. In theory, the fluorescence intensity in both FAM and HEX would be relatively weaker compared to droplets containing only  $\alpha$ -deletion (upper left quadrant) or  $\beta$ -deletion transcripts (lower right quadrant), as the availability of substrates for PCR amplification in the droplet is limited. On the other hand, in the latter case, the fluorescence intensity of double-positive droplets would be stronger, not only because each round of PCR can hydrolyze both probes but also

because the PCR template is shorter due to the double deletion, resulting in increased PCR amplification efficiency. Therefore, we conducted experiments with both cloned  $\alpha$ -deletion and  $\beta$ -deletion plasmids as template (Figure 3A and 3C) in comparison with the data obtained with cloned  $\alpha$ & $\beta$  double deletion plasmids alone as template (Figure 2C) and with all four cloned fragments together (Figure 3D). As shown in Figure 3A and 3C, the fluorescence intensity of the droplets containing both single  $\alpha$ -deletion and single  $\beta$ -deletion in the upper-right quadrant (between the dashed parallel lines) were much weaker compared to that with  $\alpha$ & $\beta$  double deletion as seen in the same quadrants of Figure 2C and Figure

3D (dashed rectangle). The large differences in signal intensity between the co-presence of  $\alpha$ - and  $\beta$ -deletions and the  $\alpha$ & $\beta$  double deletion assure that only  $\alpha$ & $\beta$  double deletion droplets at the upper right corner were counted for the tested cell samples. Read counts for each of the four cloned control templates in the various mixtures shown as 2-D displays in Figure 3 are presented in Table 1. While the molar ratios of the constructs in each mixture had not been determined prior to ddPCR, the same amount for each construct was added to the mixtures, and it is apparent that the counts for each variant are consistent among the different mixtures. As for the counts of  $\alpha$ & $\beta$  double deletion and of co-presence,

**Table 1: Calculated copies for each cloned hTERT construct and counts for the co-presence of  $\alpha$ - and  $\beta$ -deletion constructs per ddPCR reaction as shown in Figure 3.**

Mix of cloned variants	$\alpha$ -deletion	$\beta$ -deletion	Non-deletion	Double-positive droplets	
				Double-deletion	Co-presence
$\alpha$ - $\beta$ + and $\alpha$ +/ $\beta$ -	1392	4580	36	2	202
$\alpha$ - $\beta$ + and $\alpha$ +/ $\beta$ +	1392	3	2098	0	0
$\alpha$ - $\beta$ + and $\alpha$ +/ $\beta$ - and $\alpha$ +/ $\beta$ +	1258	4460	1774	0	192
$\alpha$ - $\beta$ + and $\alpha$ +/ $\beta$ - and $\alpha$ +/ $\beta$ +	1354	4140	1874	108	182

Values are from a single measurement.

these two populations of double-positive droplets can be effectively separated and then accurately counted individually. Furthermore, hTERT expression levels are generally low in tissue or cell samples. It is shown in Figure 4D that the presence of both  $\beta$ -deletion and non- $\beta$  deletion transcripts (the two most abundant hTERT splice forms in all the cells) in the same droplet is very rare (<0.1%), even though SAOS2 cells have the highest expression levels of hTERT among all the cells tested. Therefore, the number of droplets containing both the  $\alpha$ - and  $\beta$ -deletion forms would be even lower. It is most likely that the detected double-positive droplets in the upper right corners of the upper right quadrants in Figure 4B and 4C contain  $\alpha$ & $\beta$  double deletion transcripts.

After normalization against GAPDH expression, this method permits the accurate comparison of  $\alpha$ -deletion,  $\beta$ -deletion,  $\alpha$ & $\beta$  double deletions, non-deletion, and total hTERT expression among different samples (Table 2). SAOS-2 cells expressed the highest levels of total hTERT, double deletion, and  $\beta$ -deletion forms, whereas HEC-1-A cells expressed the highest percentage of  $\alpha$ -deletion amongst all cell lines tested. Although U2OS, a cell line that maintains its telomere length through an alternative lengthening mechanism, has been shown to lack telomerase activity (16),

we detected expression of extremely low levels of  $\beta$ -deletion and non-deletion forms, indicating the high sensitivity of the method. The lack of telomerase activity in the U2OS cells is actually due to the lack of hTERC expression, the RNA template component of the telomerase complex (unpublished observation with ddPCR), as has been found in several other cell lines depending on the alternative lengthening mechanism (17).

Most importantly, this method allows direct comparison of expression levels among the four spliced forms. As shown in Figure 4B, the  $\alpha$ -deletion form from HEC-1-A cells has relatively higher expression compared to the  $\beta$ -deletion transcript in OVCAR-3 cells (Figure 4C). The double deletion transcript in the OVCAR-3 cells relative to the  $\alpha$ -deletion form is higher than in HEC-1-A cells. The expression profile of MCF-7 cells obtained in the present study, with  $\alpha$ -deletion at 1.87%,  $\beta$ -deletion at 63.50%, double deletion at 2.79%, and non-deletion at 31.85% (Table 2), is strikingly similar to data previously reported using qPCR (estimated at 3.5%, 62.5%, 3.0%, and 31.5%, respectively) (13). To the best of our knowledge, our ddPCR method is the first to provide a simple, accurate and absolute quantification of four alternatively spliced transcripts for the detection of single

as well as double deletions simultaneously for direct comparison. The new method not only prevents any experimental errors that may be introduced by pipetting, but also eliminates concerns regarding PCR amplification efficiency. It should be noted that when the expression levels are high, precautions should be taken and appropriate dilutions of template/sample should be performed. On the other hand, when gene expression levels are very low, ddPCR amplification conditions, including primer design, should be optimized to avoid non-specific amplification and obtain accurate counts for each variant.

### Author contributions

B.S. and L.T. performed the experiments. B.S. and Y.L.Z. designed the study, analyzed the results, and wrote the manuscript.

### Acknowledgments

Research in Y.L.Z.'s laboratory is supported by grants from the National Cancer Institute of the National Institutes of Health (R01CA132996) and Susan G. Komen for the Cure (KG100283). The content is solely the responsibility of the authors and does not necessarily represent the official views of the funding agencies. This paper is subject to the NIH Public Access Policy.

**Table 2. The expression of four alternative spliced hTERT transcripts in cell lines relative to GAPDH and to total hTERT expression.**

Cell line	Expression relative to GAPDH ( $\times 1000$ )								Total hTERT (Average)	Average percentage of total hTERT expression			
	$\alpha$ -deletion		$\beta$ -deletion		Double-deletion		Non-deletion			$\alpha$ -deletion	$\beta$ -deletion	Double-deletion	Non-deletion
	Experiment 1	Experiment 2	Experiment 1	Experiment 2	Experiment 1	Experiment 2	Experiment 1	Experiment 2					
SAOS-2	42.77	51.40	3721.38	3615.18	238.81	267.25	1059.19	1040.33	5018.16	0.94	73.10	5.04	20.92
U2OS	0.00	0.01	14.07	13.79	0.74	0.70	8.78	9.07	23.58	0.00	59.08	3.07	37.85
WI-38	0.00	0.00	1.42	1.46	0.00	0.00	0.54	0.39	1.91	0.00	75.44	0.00	24.56
HEC-1-A	38.81	36.40	159.98	164.90	14.56	14.14	631.09	613.04	836.46	4.50	19.42	1.72	74.37
OVCAR-3	25.36	20.83	846.61	712.47	41.32	50.46	315.98	555.53	1284.28	1.80	60.70	3.57	33.93
MCF-7	18.87	22.78	756.34	661.42	31.03	31.20	354.08	356.91	1116.33	1.87	63.50	2.79	31.85

Values are the mean of duplicate measurements.

## Competing interests

The authors declare no competing interests.

## References

1. **Matlin, A.J., F. Clark, and C.W.J. Smith.** 2005. Understanding alternative splicing: towards a cellular code. *Nat. Rev. Mol. Cell Biol.* 6:386-398.
2. **Faustino, N.A. and T.A. Cooper.** 2003. Pre-mRNA splicing and human disease. *Genes Dev.* 17:419-437.
3. **Cáceres, J.F. and A.R. Kornblihtt.** 2002. Alternative splicing: multiple control mechanisms and involvement in human disease. *Trends Genet.* 18:186-193.
4. **Ulaner, G.A., J.F. Hu, T.H. Vu, L.C. Giudice, and A.R. Hoffman.** 1998. Telomerase activity in human development is regulated by human telomerase reverse transcriptase (hTERT) transcription and by alternate splicing of hTERT transcripts. *Cancer Res.* 58:4168-4172.
5. **Colgin, L.M., C. Wilkinson, A. Englezou, A. Kilian, M.O. Robinson, and R.R. Reddel.** 2000. The hTERT $\alpha$  splice variant is a dominant negative inhibitor of telomerase activity. *Neoplasia* 2:426-432.
6. **Listerman, I., J. Sun, F.S. Gazzaniga, J.L. Lukas, and E.H. Blackburn.** 2013. The major reverse transcriptase-incompetent splice variant of the human telomerase protein inhibits telomerase activity but protects from apoptosis. *Cancer Res.* 73:2817-2828.
7. **Lincz, L.F., L.M. Mudge, F.E. Scorgie, J.A. Sakoff, C.S. Hamilton, and M. Seldon.** 2008. Quantification of hTERT splice variants in melanoma by SYBR green real-time polymerase chain reaction indicates a negative regulatory role for the beta deletion variant. *Neoplasia* 10:1131-1137.
8. **Liu, Y., B.Q. Wu, H.H. Zhong, X.X. Tian, and W.G. Fang.** 2012. Quantification of alternative splicing variants of human telomerase reverse transcriptase and correlations with telomerase activity in lung cancer. *PLoS ONE* 7:e38868. Electronic Resource.
9. **Fujiwara-Akita, H., C. Maesawa, T. Honda, S. Kobayashi, and T. Masuda.** 2005. Expression of human telomerase reverse transcriptase splice variants is well correlated with low telomerase activity in osteosarcoma cell lines. *Int. J. Oncol.* 26:1009-1016.
10. **Zaffaroni, N., R. Villa, U. Pastorino, R. Cirincione, M. Incarbone, M. Alloisio, M. Curto, S. Pilotti, and M.G. Daidone.** 2005. Lack of telomerase activity in lung carcinoids is dependent on human telomerase reverse transcriptase transcription and alternative splicing and is associated with long telomeres. *Clin. Cancer Res.* 11:2832-2839.
11. **Yi, X., J.W. Shay, and W.E. Wright.** 2001. Quantitation of telomerase components and hTERT mRNA splicing patterns in immortal human cells. *Nucleic Acids Res.* 29:4818-4825.
12. **Ohyashiki, J.H., H. Hisatomi, K. Nagao, S. Honda, T. Takaku, Y. Zhang, G. Sashida, and K. Ohyashiki.** 2005. Quantitative relationship between functionally active telomerase and major telomerase components (hTERT and hTR) in acute leukaemia cells. *Br. J. Cancer* 92:1942-1947.
13. **Mavrogianou, E., A. Strati, A. Stathopoulou, E.G. Tsaroucha, L. Kaklamanis, and E.S. Lianidou.** 2007. Real-time RT-PCR quantification of human telomerase reverse transcriptase splice variants in tumor cell lines and non-small cell lung cancer. *Clin. Chem.* 53:53-61.
14. **Hara, T., T. Noma, Y. Yamashiro, K. Naito, and A. Nakazawa.** 2001. Quantitative analysis of telomerase activity and telomerase reverse transcriptase expression in renal cell carcinoma. *Urol. Res.* 29:1-6.
15. **Hindson, B.J., K.D. Ness, D.A. Masquelier, P. Belgrader, N.J. Heredia, A.J. Makarewicz, I.J. Bright, M.Y. Lucero, et al.** 2011. High-throughput droplet digital PCR system for absolute quantitation of DNA copy number. *Anal. Chem.* 83:8604-8610.
16. **Ulaner, G.A., J.F. Hu, T.H. Vu, H. Oruganti, L.C. Giudice, and A.R. Hoffman.** 2000. Regulation of telomerase by alternate splicing of human telomerase reverse transcriptase (hTERT) in normal and neoplastic ovary, endometrium and myometrium. *Int. J. Cancer* 85:330-335.
17. **Hoare, S.F., L.A. Bryce, G.B.A. Wisman, S. Burns, J.J. Going, A.G.J. van der Zee, and W.N. Keith.** 2001. Lock of telomerase RNA gene hTERC expression in alternative lengthening of telomere cells is associated with methylation of the hTERC promoter. *Cancer Res.* 61:27-32.

Received 26 January 2014; accepted 05 May 2014.

Address correspondence to Yun-Ling Zheng, Cancer Prevention and Control Program, Lombardi Comprehensive Cancer Center, Georgetown University Medical Center, Washington, DC. E-mail: yz37@georgetown.edu

To purchase reprints of this article, contact: [biotechniques@fosterprinting.com](mailto:biotechniques@fosterprinting.com)

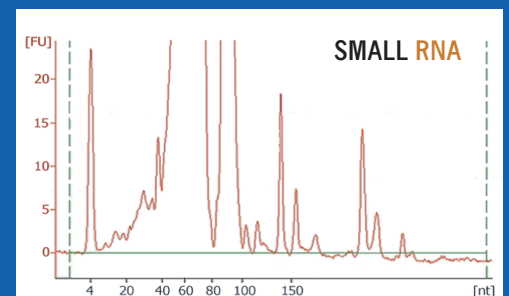
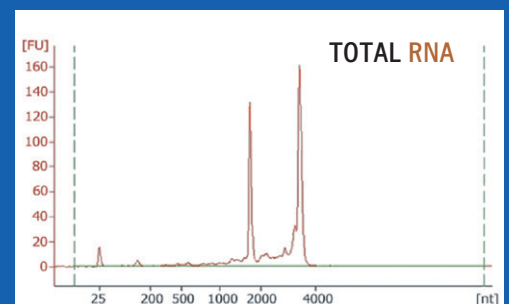
# A NEW STANDARD IN RNA ISOLATION

## RNAzol<sup>®</sup> RT\*

Isolates total RNA, with mRNA and small RNA (200-10 bases) in separate fraction

- ▶ The single-step method without phase separation
- ▶ No DNase treatment necessary
- ▶ RNA ready for RT-PCR, microarrays and other applications
- ▶ No need for refrigerated centrifuge
- ▶ One reagent for solid and liquid samples

THE HIGHEST YIELD AND PURITY:



[www.mrcgene.com](http://www.mrcgene.com) (888) 841-0900

\* Piotr Chomczynski, US patent 2010

MOLECULAR RESEARCH CENTER INC.

RNAzol is a trademark of Molecular Research Center, Inc